

Modelling sea level surges in the Firth of Clyde, a fjordic embayment in south-west Scotland

Alessandro D. Sabatino¹  · Rory B. O'Hara Murray² · Alan Hills³ · Douglas C. Speirs¹ · Michael R. Heath¹

Received: 14 January 2016 / Accepted: 24 July 2016 / Published online: 12 August 2016
© The Author(s) 2016. This article is published with open access at Springerlink.com

Abstract Storm surges are an abnormal enhancement of the water level in response to weather perturbations. They have the capacity to cause damaging flooding of coastal regions, especially when they coincide with astronomical high spring tides. Some areas of the UK have suffered particularly damaging surge events, and the Firth of Clyde is a region with high risk due to its location and morphology. Here, we use a three-dimensional high spatial resolution hydrodynamic model to simulate the local bathymetric and morphological enhancement of surge in the Clyde, and disaggregate the effects of far-field atmospheric pressure distribution and local scale wind forcing of surges. A climatological analysis, based on 30 years of data from Millport tide gauges, is also discussed. The results suggest that floods are not only caused by extreme surge events, but also by the coupling of spring high tides with moderate surges. Water level is also enhanced by a funnelling effect due to the bathymetry and the morphology of fjordic sealochs and the River Clyde Estuary. In a world of rising sea level, studying the propagation and the climatology of surges and high water events is fundamental. In addition, high-resolution hydrodynamic models are essential to forecast extreme events and to prevent the loss of lives, or to plan coastal defences solutions.

Keywords Surge · Flooding · Ocean modelling · Clyde Sea · Fjordic basin

Electronic supplementary material The online version of this article (doi:[10.1007/s11069-016-2506-7](https://doi.org/10.1007/s11069-016-2506-7)) contains supplementary material, which is available to authorized users.

✉ Alessandro D. Sabatino
alessandro.sabatino@strath.ac.uk

¹ Marine Population Modelling Group, Department of Mathematics and Statistics, University of Strathclyde, Glasgow, UK

² Marine Scotland Science, Marine Laboratory, Aberdeen, UK

³ SEPA, Scottish Environment Protection Agency, Eurocentral, Holytown, UK

1 Introduction

Storm surges are a tsunami-like sea level perturbation due to extreme low- or high-pressure weather systems, causing an enhancement or a decrease in the sea level at the coastline compared to the usual astronomical tides. When this change is positive, surges threaten coastal communities, causing floods and damage to coastal infrastructures, and occasionally claiming the lives of people. The most dangerous situation is when a surge wave coincides with a spring tide high water event.

Surges are a threat to coastal communities in Scotland (Werritty et al. 2007). In particular, this study is focused on the surges affecting some areas of the Clyde Sea, in the south-west of Scotland. This area has been struck by several floods due to storm surges, since the well-documented massive surge of 1953 (Hickey 2001), such as the 5th January 1991 event that caused extensive flooding and damage estimated as £7 M (Kaya et al. 2005). In the aftermath, a pilot study was appointed to estimate the economic damage due to storm surge (Townson and Collar 1993). Subsequently, the Scottish Environmental Protection Agency (SEPA) commissioned an Early Warning system for flooding events, including the development of a hydrodynamic model (Kaya et al. 2005) for forecasting dangerous surge events, which are estimated to cause £0.45 M per year damage.

In contrast to south-west Scotland, coastal communities in Northern Ireland separated from Scotland by the North Channel are less exposed to flooding risk caused by storm surge events (Hankin et al. 2008). A statistical study (Orford and Murdy 2015) highlighted that the majority of the large surges that have been recorded in Belfast Lough were caused by westerly winds, associated with the positive North Atlantic Oscillation (NAO) phase, while only 20 % of the largest surge were caused during the negative NAO phase.

The Clyde Sea is a semienclosed fjordic basin and is connected to the North Atlantic Ocean and to the Irish Sea through the North Channel (Fig. 1). Matthews et al. (1999) divided the Clyde Sea in two main regions: the inner Clyde, which comprises the various sealochs and the Clyde Estuary, which are most influenced by the freshwater input and contain deep areas, and secondly, the outer Firth that is the wide and shallow sea area that communicates with the North Channel and is more influenced by the ocean climate. The tidal motion of the region is mainly driven by the M_2 amphidrome, situated north of the Clyde Sea, near the Isle of Mull (Pingree and Griffiths 1979). Due to the amphidrome, the bathymetry and the coastline, maximum tidal currents in the Inner Clyde Sea are less than 0.4 m/s, while those in the North Channel exceed 1.4 m/s (Dietrich 1950). The main consequence is that the Clyde Sea shows a strong stratification (Pingree et al. 1978), while the North Channel is well mixed since the bottom layer occupies all of the water column (Davies et al. 2004).

Although the Clyde Sea and the North Channel have been well studied with respect to tidal-driven (Davies and Hall 1998), wind-driven (Davies and Hall 2000; Davies et al. 2001) and stratification-driven (Simpson and Rippeth 1993; Rippeth and Simpson 1996) circulation, surge propagation and internal generation of surge waves in the Clyde Sea are not well studied. These two features are the focus of this paper, together with the climatology of the storm surges.

Here, we explore three storm surges in December 2011 (8–9, 13 and 28 December 2011). December 2011 was one of the stormiest months on record for Scotland. The storm surge on the 8–9 December 2011 (Storm Friedhelm, nicknamed by the British press as Hurricane *Bawbag*) caused severe flooding on all the west coast of the UK, from Cumbria to the Orkneys island, causing an estimated £100 M of damages in Scotland alone. In Ayr,

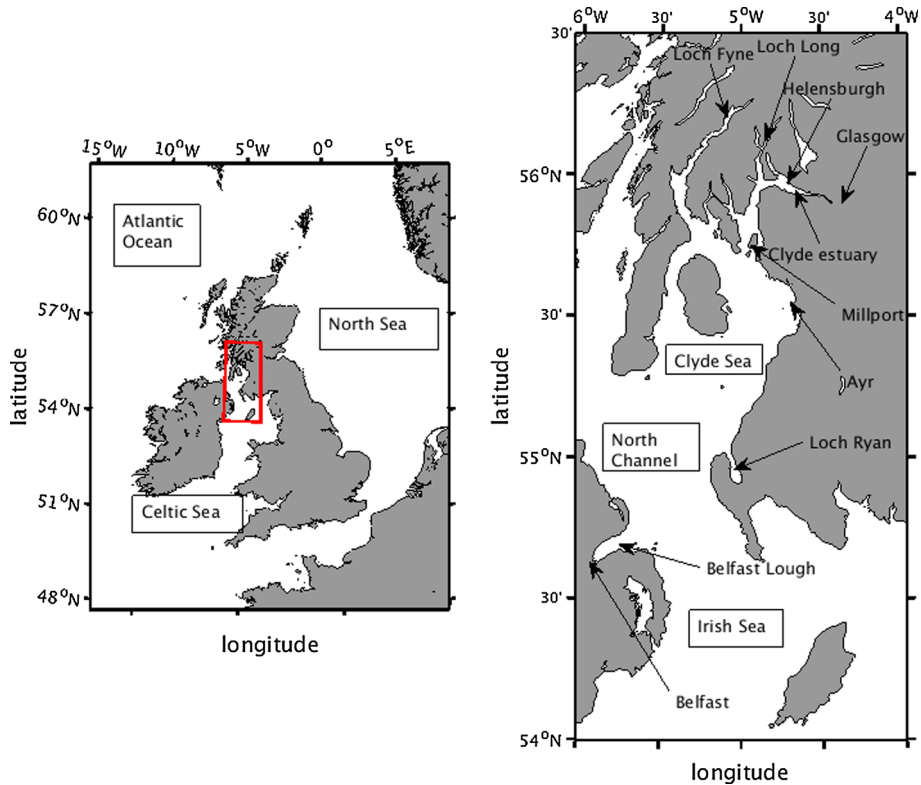


Fig. 1 Position of the Clyde Sea and the North Channel in the Great Britain Islands. Main places cited in the paper are shown

the maximum recorded wind gust during the storm exceeded 36 m/s. The 13 December and the 28 December surges flooded part of the town of Helensburgh, situated between Gare Loch and the Clyde Estuary. Helensburgh (about 15,000 inhabitants) is often flooded in severe surge conditions or when mild or strong surges are coupled with spring tide conditions. Figure 2 shows some pictures taken on the 28 December 2011 in Helensburgh: coastal defences were overwhelmed, and the marina, the pier, and the streets near the coastline were flooded.

2 Methods

2.1 The hydrodynamic model

The water circulation of the Clyde Sea and the North Channel was simulated using Finite-Volume Community Ocean Model (FVCOM), which was developed by Chen et al. (2003) mainly for simulating the flow of complex shelf and estuarine areas. FVCOM was later updated by a joint team from Woods Hole and the University of Massachusetts (Chen et al. 2006). FVCOM has been applied successfully for surge forecast and hindcast purposes. In particular, it was modified for the hindcast of hurricane-generated storm surges (Rego and



Fig. 2 Images from the 28 December 2011 storm in Helensburgh (Photos Joanna Heath)

Li (2009b): Rego and Li (2009a) modelled the effect of hurricanes-induced storm surge on the low-lying coastline of Louisiana, while Weisberg and Zheng (2008) used an FVCOM model for studying the effect of an Ivan-like hurricane on Florida coastline. The effects on the coastline of Texas of the storm surge wave induced by Hurricanes Rita and Ike were studied by Rego and Li (2010a, b). The FVCOM model is based on the numerical solution of primitive equations in 3-D. The model equations in Cartesian, sigma-layers coordinates are reported in Chen et al. (2003). The model solves the equations on an unstructured grid using a finite-volume approach (Versteeg and Malalasekera 2007), optimized for parallelization on a MPI cluster (Cowles 2008). Horizontal and vertical closure of the governing equation was made with a default setup of the $k - \epsilon$ model and Smagorinsky turbulent closure schemes for vertical and horizontal mixing, respectively (Rodi 1993; Smagorinsky 1963).

2.2 Model forcings

Various datasets were used to force the model. Tidal boundary conditions were extracted from the European Shelf OTPS local solution (Egbert et al. 2010), an open-source software for tidal predictions based on the TOPEX/Poseidon satellite data observations and on tidal harmonic components from the major ports. To account for storm surges generated outside the model domain, residuals were extracted from the tide gauges closest to the model boundary and added to the tidal elevations (Table 1). Tide gauge data were from the UK tide gauge network and were provided by the British Oceanographic Data Centre (BODC) and by the Scottish Environmental Protection Agency (SEPA). For simulating surges generated internally in the model domain, wind and pressure fields were provided to the hydrodynamical model from the ERA-Interim dataset (Dee et al. 2011) at a time resolution of 3 h and a spatial resolution of $0.125^\circ \times 0.125^\circ$. The ERA-Interim data were covering

Table 1 List of tide gauges used for the estimation of the residuals

| Tide gauge | Latitude (°) | Longitude (°) |
|-------------------|--------------|---------------|
| Southern boundary | | |
| Holyhead | 53.308 | −4.631 |
| Workington | 54.651 | −3.568 |
| Llandudno | 53.332 | −3.825 |
| Port Erin* | 54.09 | −4.77 |
| Northern boundary | | |
| Tobemory | 56.623 | −6.064 |
| Port Rush* | 55.206 | −6.657 |
| Port Ellen* | 55.63 | −6.19 |

* Those tide gauges are inside the model boundary and were also used for the validation of the model

Table 2 Location and properties of the river data provided by Scottish Environmental Protection Agency (SEPA)

| Name | Station | Lat (°) | Lon (°) | Catchment (km ²) | Mean flow (m ³ /s) | Max flow (m ³ /s) |
|----------------|--------------|---------|---------|------------------------------|-------------------------------|------------------------------|
| Doon | Auchendrane | 55.410 | −4.627 | 323.8 | 7.641 | – |
| Stinchar | Balnowlart | 55.107 | −4.968 | 341 | 10.713 | 177 |
| Clyde | Daldowie | 55.830 | −4.122 | 1903.1 | 48.192 | 464.81 |
| Little Eichaig | Dalinlongart | 55.995 | −4.980 | 30.8 | 1.789 | 13.04 |
| Carradale | Dippen | 55.583 | −5.497 | 58.5 | 2.476 | – |
| Ayr | Mainholm | 55.461 | −4.593 | 574 | 15.943 | 231.08 |
| Girvan | Robstone | 55.259 | −4.808 | 245.5 | 6.788 | 63.592 |
| Irvine | Shewalton | 55.597 | −4.628 | 380.7 | 9.689 | 324.43 |

the 2002–2011 period, in which the simulations were carried out. To evaluate river contribution to surge events in the Clyde Sea, eight rivers were included in the model. River discharge informations for the period 2005–2011 were provided by SEPA with a 15-min resolution. The locations and main features of those rivers are reported in Table 2.

The implementation of the model forcings was made using MATLAB, modifying the FVCOM MATLAB toolbox developed by Geoffrey Cowles and Pierre Cazenave. The results were plotted using MATLAB *m_map* toolbox (Pawlowicz 2000). Although the model can run in baroclinic, the outputs showed in this paper are all from barotropic run.

2.3 Calibration and validation procedure

The model was calibrated using the water elevation recorded by the tide gauge data from Millport in 2007 for 11 months (the first month was considered spin-up time). After the calibration, the model was run for the whole of the year 2003 and then validated (first month, December 2002: spin-up time) by two different methods.

Firstly, the model was validated by extracting the water level harmonic components (Codiga 2011) and comparing these with the recorded tide gauge. The performance of the

Table 3 Position of the tide gauges used for the validation of the model

| Tide gauge | Tide gauge name | Latitude | Longitude | Provided by |
|------------|-----------------|----------|-----------|-------------|
| A | Rothesay | 55.84 | −5.05 | SEPA |
| B | Girvan | 55.24 | −4.87 | SEPA |
| C | Tarbert | 55.86 | −5.41 | SEPA |
| D | Portrush | 55.21 | −6.66 | BODC |
| E | Port Erin | 54.09 | −4.77 | BODC |
| F | Port Ellen | 55.63 | −6.19 | BODC |
| G | Portpatrick | 54.84 | −5.12 | BODC |
| H | Bangor | 54.66 | −5.67 | BODC |
| I | Millport | 55.75 | −4.91 | BODC |
| J | Campbeltown | 55.43 | −5.60 | SEPA |

model was assessed by calculating the root-mean-square error based on the harmonic components extracted from all the tide gauges reported in Table 3. This first method was carried out to assure that the model reproduced the tidal wave propagation in the Clyde Sea.

Secondly, the model was validated for the total water level, in order to evaluate the agreement between the recorded and the hindcast water level due to surge and tides. In this case, this validation was based on the reproduction of residual elevations at the boundaries. We used five different tide gauges at various locations in the domain. Four different statistical indices were used for the validation:

$$\text{Bias} = \frac{1}{N} \sum_{i=1}^N (x_{oi} - x_{mi}) \tag{1}$$

$$\text{RMSE} = \sqrt{\frac{1}{N} \sum_{i=1}^N (x_{oi} - x_{mi})^2} \tag{2}$$

$$\text{NRMSE} = \frac{\text{RMSE}}{\max(x) - \min(x)} \tag{3}$$

$$R^2 = \left(\frac{\sum_{i=1}^N (x_{oi} - \bar{x}_o)(x_{mi} - \bar{x}_m)}{\sqrt{\sum_{i=1}^N (x_{oi} - \bar{x}_o)^2 (x_{mi} - \bar{x}_m)^2}} \right)^2 \tag{4}$$

The bias is used to assess if there are some significant, the root-mean-square error (RMSE) represent the sample standard deviation between observed and modelled values, the normalized root-mean-square error (NMRSE) is used to understand the percentage significance of the RMSE on the total water level, while the R^2 is the Pearson correlation coefficient that measures the linear correlation between the modelled and the observed values. For the analysis of the surge residuals, also the standard deviation σ of the total water level has been used. The expression of σ is the same as the root-mean-square (RMSE).

Water levels at tide gauges were provided by the British Oceanographic Data Center (BODC) and by the Scottish Environmental Protection Agency (SEPA).

2.4 Surge historical analysis

For the surge historical analysis of the Clyde Sea, the tide gauge data from Millport was available for a 30-year period (1985–2014), from British Oceanographic Data Center (BODC), including both total water level and residuals. Storms that generated the surge wave were tracked using wind (m/s) and pressure (Pa) data from ECMWF ERA-Interim reanalysis (Dee et al. 2011), at a time resolution of 3 hours and a spatial resolution of $0.125^\circ \times 0.125^\circ$ from 1985 to 2014.

Using the Millport tide gauge, we identified the largest surges based on the residuals. Storms with residuals exceeding 1 m were considered. Storms were classified into five different categories, depending on the path and the evolution of the storm from ERA-Interim data.

Since residuals are often not associated with spring high water events, at Millport, the standard deviation of the total water level was estimated and the events exceeding 2σ and 3σ were identified as potentially damaging surge events, and the distribution of the residuals with the astronomical tidal elevation was studied.

2.5 Grid generation

Generation of the computational grid for the Clyde Sea and for the North Channel followed the guidelines reported in the FVCOM User manual (Chen et al. 2006). Since no grid generator was included in the code, the SMS grid generator was used (Aquaveo 2007; Banks et al. 2014) to create the computational mesh. FVCOM adopts an unstructured grid approach, with triangular elements (Ferziger and Perić 2002). Unstructured grids can represent complex coastlines better than rectangular grids and potentially provide more realistic flows, enabling the geography of the coastline to affect the propagation of tidal and surface waves in a realistic manner. FVCOM has some quality requirements for the computational mesh. In particular, it should meet these requirements:

- Minimum interior angle of each element: 30°
- Maximum interior angle of each element: 120°
- Maximum slope: 0.1
- Element area change: 0.5
- Connecting elements: should be less than 8 for each node

The grid was generated using the Global Self-consistent, Hierarchical, High-resolution Geography Database (GSHHG) coastline from NOAA (Wessel and Smith 1996), joint with the SeaZone high-resolution coastline for the internal areas of the Clyde Sea. Bathymetric information was, then, interpolated on the grid using SMS. The bathymetry used was the GEBCO (Fisher et al. 1982) with a spatial resolution of 30 arc second, interpolated with the high-resolution bathymetry from SeaZone. Figure 3 shows the computational grid used for this study. The grid was generated with the boundaries far away from the area of study. This avoids boundary noise influencing the circulation in the study area and reduces the issue of unphysical speeds or water elevations within the Clyde Sea domain. The resolution varies between 5 km at the open ocean boundaries to <100 m in lochs, such as Loch Fyne and the area of the Clyde Estuary.

2.6 December 2011 storms

ERA-Interim datasets were used to hindcast pressure conditions during the three storms that occurred in December 2011. Between 8 and 9 December 2011 Britain experienced an

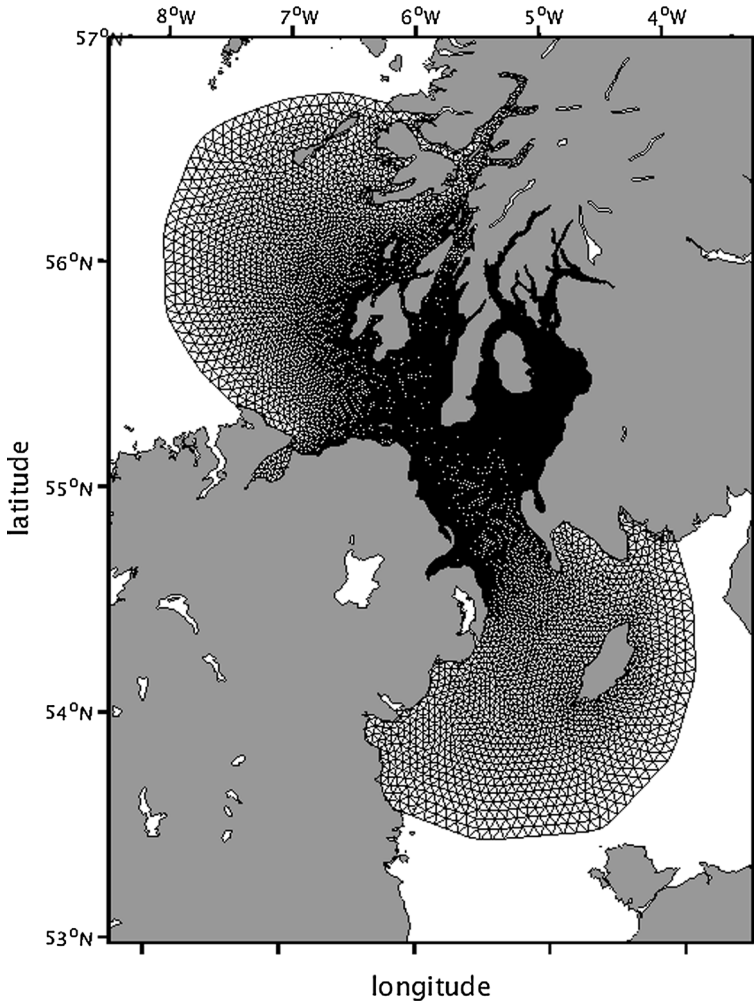


Fig. 3 Computational grid generated with SMS used for the FVCOM Clyde Sea model

extremely intense extratropical cyclone, with hurricane-force winds hitting Scotland and Northern England. Wind gusts exceeding 42 m/s were reported, causing widespread damage. The extratropical cyclone was nicknamed by the British press Hurricane Bawbag. Figure 4 shows the evolution of the storm between 8 and 9 December 2011 over Great Britain. The storm was formed in the North Atlantic Ocean and moved quickly to Scotland. On the 8 December at 12:00 UTC, the pressure minimum was 957 hPa, with maximum sustained wind gusts at surface exceeding 47 m/s. At the 9 December at 00:00 UTC, the minimum was over the North Sea, passing through Orkney-Fair Isle channel.

A few days later, a strong depression formed over the North Atlantic Ocean, with a pressure minimum less than 945 hPa, that was the lowest recorded pressure in UK since 2000. Figure 5 shows the evolution of Cyclone Hergen. The path and the evolution of this cyclone was very similar to the Hurricane Bawbag, generating a very large storm surge where the residuals exceeded 1 m in Millport, flooding Helensburgh and other towns in the

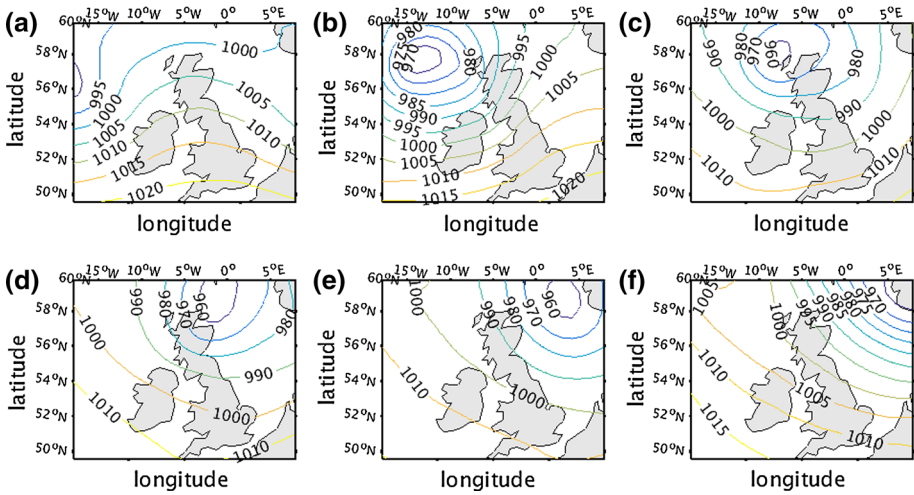


Fig. 4 Evolution of the mean sea level pressure (hPa) during Hurricane Bowbag from 8 December 2011 00:00 UTC. The pressure field is plotted every 6 h: **a** 08/12/2010 00:00 UTC, **b** 08/12/2010 06:00 UTC, **c** 08/12/2010 12:00 UTC, **d** 08/12/2010 18:00 UTC, **e** 09/12/2010 00:00 UTC and **f** 09/12/2010 06:00 UTC

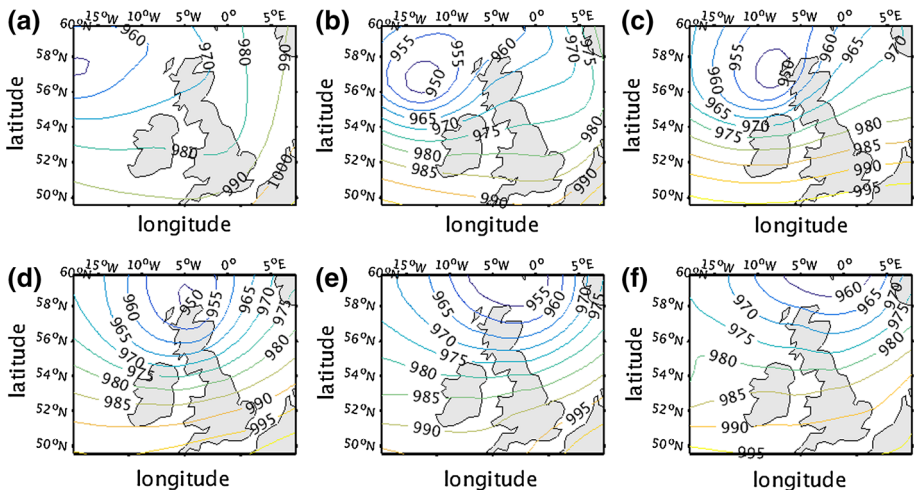


Fig. 5 Evolution of the mean sea level pressure (hPa) during the Cyclone Hergen from 13 December 2011 00:00 UTC. The pressure field is plotted every 6 h: **a** 13/12/2010 00:00 UTC, **b** 13/12/2010 06:00 UTC, **c** 13/12/2010 12:00 UTC, **d** 13/12/2010 18:00 UTC, **e** 14/12/2010 00:00 UTC and **f** 14/12/2010 06:00 UTC

Clyde Sea. The M4 weather buoy of the Marine Ireland, off the Donegal coast recorded a surface wave with a height of 20.4 m.

The last storm considered in this study occurred on the 28 December 2011 and generated a surge wave that in Millport exceeded 0.7 m. The storm followed the same path of the other two previous storms, with the low pressure in the North Atlantic Ocean moving to Orkneys-Fair Isle channel. In this storm, however, the pressure minimum was less intense, and the damages were less than the other two (Fig. 6).

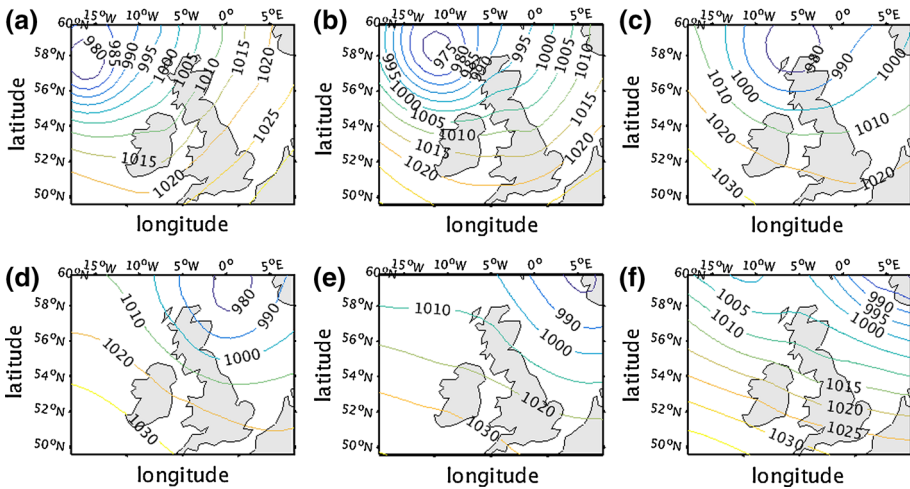


Fig. 6 Evolution of the mean sea level pressure (hPa) during the 28 December storm from 00:00 UTC. The pressure field is plotted every 6 h: **a** 28/12/2010 00:00 UTC, **b** 28/12/2010 06:00 UTC, **c** 28/12/2010 12:00 UTC, **d** 28/12/2010 18:00 UTC, **e** 29/12/2010 00:00 UTC and **f** 29/12/2010 06:00 UTC

3 Results

3.1 Surge climatology of the Clyde Sea

Between 1985 and 2014, the Millport tide gauge recorded 92 surge events that exceeded 1 m. Sources of storm were classified into five main categories (Table 4), depending on the position of the low pressure minimum that caused the storm surge (Table S1 of the supporting material provides more details of the 90 storms considered). Percentages were evaluated from the Table S1 based on the frequency of occurrence of those events in the 30 years of records in Millport. The most common pattern for a weather system causing a large surge event in the Clyde is a low-pressure system moving from the North Atlantic Ocean to, generally, the Fair Isle Channel (Table 4). In this case, the storm surge could be generated either in the open North Atlantic itself (case 1) or close to the western coastline of Scotland (case 2), depending on where the storm reaches its maximum. It is also possible for a pressure minimum from the North Atlantic Ocean to move over the Scottish mainland (north of the Clyde Sea, between 56 and 60 N) and generate a storm surge near the Clyde Sea (case 3). Severe storm surges are rarely internally generated in the Clyde: This is the case of a low-pressure system moving from the North Atlantic Ocean to Ireland and to Clyde Sea itself (case 4). In this case, the storm surge is caused in response to the local field of wind and pressure. An extremely rare case is when the wind circulation around a low-pressure system over the North Sea causes a storm surge in the Irish Sea and the Clyde Sea (case 5). Case 5 has only once been recorded, on the 31 December 2006.

Comparing results in Table 4 with the results in Table 1 of Olbert and Hartnett (2010), it is possible to see that for both for Irish water and for the Clyde Sea, the largest part of storms come from SW and pass to the north of the Clyde: The same storm events that can cause damages on Irish coastal cities can cause floodings in the Clyde Sea. However, the frequency of storms generated when the minimum is south of 55 N is very low in the Clyde

Table 4 Classification of depression that caused large storms in the Clyde Sea, compared with Table 1 in Olbert and Hartnett (2010)

| Storm group | Percentage (%) | Location | Description |
|---------------------|----------------|-----------------------|---|
| North of Scotland | 34.6 | Above 60 N | Depression over Orkneys or in the Fair Isle Channel |
| North Atlantic | 28.9 | West of 10 W | Depression over North Atlantic Ocean |
| North-West Scotland | 25.6 | Between 55 N and 60 N | Depression over Hebridian Island or North-West Scotland |
| Scotland South | 8.9 | South of 55 N | Depression over Ireland, North Channel or Clyde Sea |
| North Sea | 1.1 | East of 2 W | Depression over the North Sea |

Sea (about 9 % of the severe storms), but is about 29 % for the more southerly Irish coastline.

Figure 7 shows the climate statistics for the occurrence of storms based on the month of occurrence. As expected, the autumn–winter period (from November to February) is the stormiest period for the Clyde Sea, in which the majority of the large storm surges are recorded. However some surges exceeding 1 m in Millport are recorded also in spring and in summer months.

3.2 Extreme water level climatology of the Clyde Sea

Flooding events in the Clyde are not only connected to the extremes of surge residuals, but to the coincidence of high residuals and spring tide. The standard deviation of the total water level at Millport was evaluated, over the period 1985–2014. All the recorded elevations exceeding 2σ and 3σ were then extracted (Fig. 8). The most frequent situation for water level exceeding 2σ was when moderate surge residuals (between 0.5 and 0.8 m) occurred at the same time as spring high tide events (with water level exceeding 1.2 m, tidal range exceeding 2.2–2.4 m). Conversely, extreme events (water level $> 3\sigma$) were recorded when the residual was less than 0.5 m. Events with sea level exceeding 3σ occurred only in 7 years over the 30 analysed (about 23.3 %). As expected, there is no relation between the occurrence of severe surge and astronomical spring high tides.

3.3 Model calibration and validation

The final parameter settings of the hydrodynamic model after the calibration procedure are shown in Table 5. The results of the sea level validation are reported in Tables 6 and 7 for semidiurnal and diurnal components, respectively. The results show that the model performed well against tidal harmonic component (both semidiurnal and diurnal, Tables 6, 7, respectively). In particular, the main component in the Clyde Sea and in the North Channel is the M_2 component. Considering the results from all ten tide gauges, the Root-Mean-Square Error for the M_2 harmonic component was 1.19 cm and 7.06° for the amplitude and the phase, respectively.

Since our focus is on surge events, it is important to understand how the model agrees with the observation for total water level. In Table 8, we report the statistical comparison

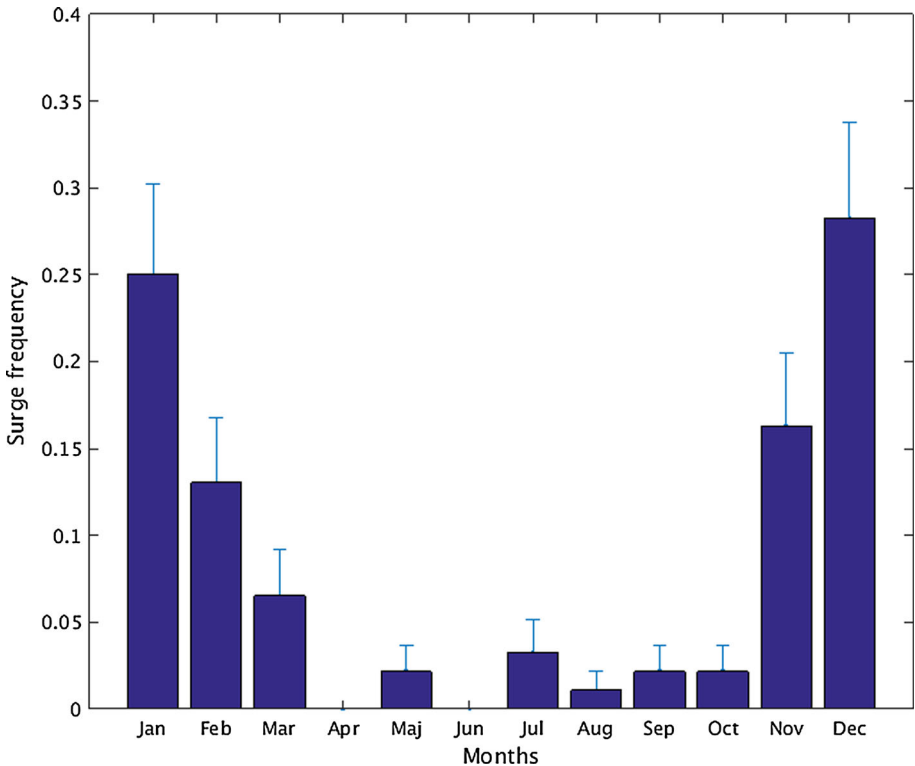


Fig. 7 Monthly frequency of the surges in Millport exceeding 1 m in the period 1985–2014. The frequency is calculated as the number of storms occurring in the month divided by the total number of storms in the record

between observed and modelled water level in different areas of the domain. The RMSE for the total water does not exceed 20 cm and 5 % of the total water level. Analysing the residuals between modelled and recorded water level, we conclude that the model underestimates the total water level (<1 cm for all the tide gauges considered).

3.4 Surge spatial statistics

Results reported here are based on the 2003 that was a relatively calm year for storm surge events (Table S1). For years like 2011, in which several surge exceeding 1 m were recorded in Millport, the results for the maximum and the average effect of the surge are larger (Figs. 9b, 10b).

Models were run with different surge forcing, in addition to tidal forcing, and each one was compared with a model run with only tidal forcing. Figure 9 shows the root-mean-square deviations (calculated as the RMSE) between each model run and the tide only simulating, with Fig. 9a showing the effect of the external surge, Fig. 9b showing the effect of the local wind and pressure fields, and Fig. 9c showing the combined external surge and local wind and pressure. Figure 10 shows the maximum effect of (a) the external surge forcing, (b) the local wind and pressure fields, and (c) the combined external and local surge. Both figures show that the amplitude of the surge wave increased towards the

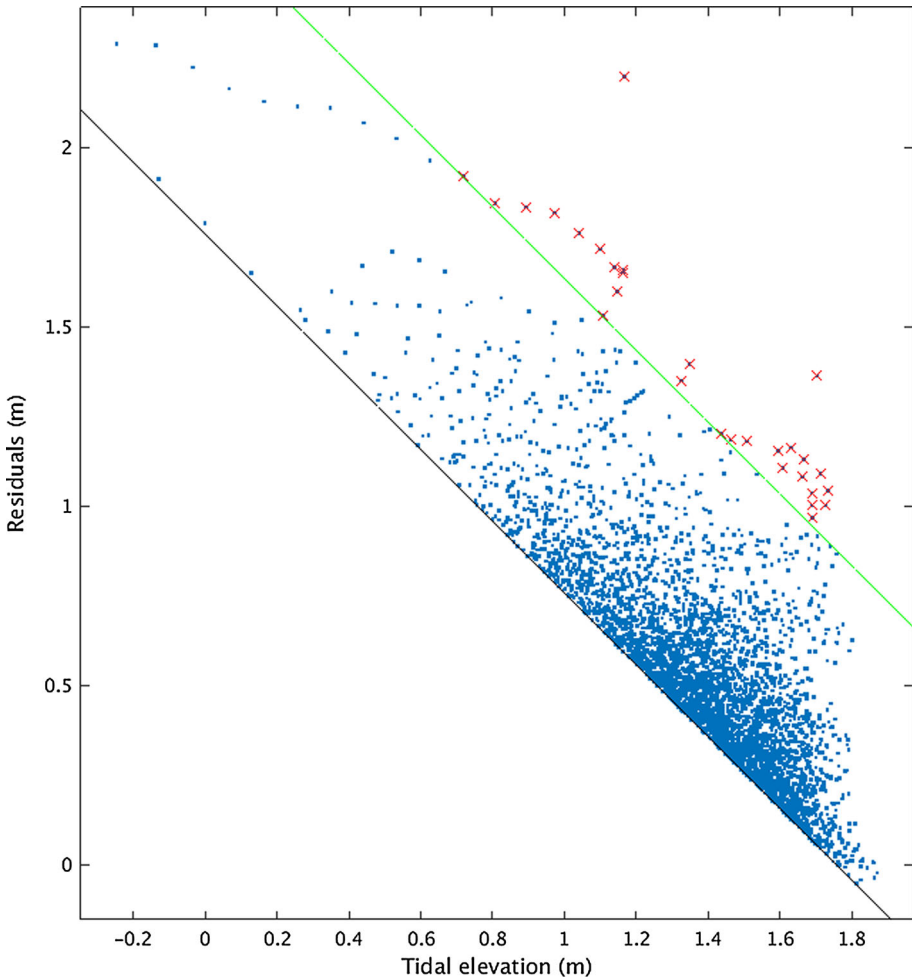


Fig. 8 Surge residuals (calculated as total water level minus the astronomical tidal contribution) versus astronomical tidal elevations for large water level events in Millport, *blue points* are recorded water level exceeding 2σ (1.75 m) in Millport, while *red crosses* are recorded water level exceeding 3σ (2.63 m). σ is the standard deviation of the water level (0.89 m). The *black* and the *green line* represent the 2σ and the 3σ respectively

fjordic areas of the Clyde Sea, located to the north of the estuary. In particular, the strongest effect in the Clyde Sea is recorded in the estuary and in Loch Fyne, with a maximum combined effect of Atlantic surge and local surge of 1.2 m. In the estuary, in particular, the surge wave can be up to 1.5 m (Fig. 10c) without considering the effect of the Clyde river discharge.

The effect of the Atlantic storms is stronger than the effect of the local wind on the surge. From the previous analysis of historical records, only 9 % of the recorded surge events at Millport exceeding 1 m were generated internally. However, in combination with the storms from outside, local conditions can significantly enhance the water level and contribute to severe surges.

Table 5 Model parameters after the calibration

| Variable | Value |
|-----------------------------|-----------|
| Timestep | 1 s |
| Smagorinsky constant | 0.4 |
| Horizontal Prandtl number | 1.0 |
| Vertical Prandtl number | 1.0 |
| Vertical mixing coefficient | 10^{-6} |
| Minimum bottom roughness | 0.0024 m |
| Roughness length | 0.001 m |
| Sponge layer | 11 km |
| Damping coefficient | 0.008 |

Table 6 Comparison of the observed and modelled amplitude and phase for dominant semidiurnal tidal components for the year 2003 h_o and g_o are the observed amplitude in cm and the phase degrees respectively and h_m and g_m are the modelled amplitude in cm and the phase degrees

| | M_2 | | | | S_2 | | | | N_2 | | | |
|---|-------|-------|-------|-------|-------|-------|-------|-------|-------|-------|-------|-------|
| | h_o | g_o | h_m | g_m | h_o | g_o | h_m | g_m | h_o | g_o | h_m | g_m |
| A | 118 | 342 | 117 | 342 | 31.8 | 35.3 | 29.4 | 38.2 | 22.2 | 315 | 20.8 | 318 |
| B | 108 | 347 | 106 | 338 | 28.9 | 40.4 | 26.4 | 33.4 | 20.5 | 321 | 18.9 | 314 |
| C | 115 | 344 | 115 | 342 | 31.2 | 37.2 | 28.8 | 38.5 | 21.7 | 317 | 20.4 | 318 |
| D | 53.1 | 199 | 54.1 | 199 | 22.7 | 212 | 24 | 211 | 11.7 | 176 | 11.8 | 171 |
| E | 184 | 322 | 184 | 323 | 56.3 | 1.55 | 54.5 | 5.81 | 35.7 | 297 | 34.1 | 299 |
| F | 15.6 | 85.7 | 15.7 | 65.4 | 13.9 | 151 | 14.6 | 150 | 2.23 | 74.4 | 2.93 | 61 |
| G | 136 | 332 | 137 | 332 | 38.4 | 16.9 | 37 | 18.4 | 25.9 | 306 | 25 | 307 |
| H | 118 | 317 | 119 | 317 | 30.4 | 0.574 | 28.4 | 0.626 | 22.5 | 291 | 21.3 | 291 |
| I | 113 | 342 | 115 | 341 | 30.5 | 34.7 | 28.9 | 37.7 | 21.7 | 317 | 20.5 | 317 |
| J | 105 | 344 | 104 | 344 | 28.1 | 36.7 | 25.8 | 41.1 | 20 | 317 | 18.5 | 320 |

Table 7 Comparison of the observed and modelled amplitude and phase for dominant diurnal tidal components for the year 2003 h_o and g_o are the observed amplitude in cm and the phase degrees respectively and h_m and g_m are the modelled amplitude in cm and the phase degrees

| | K_1 | | | | O_1 | | | |
|---|-------|-------|-------|-------|-------|-------|-------|-------|
| | h_o | g_o | h_m | g_m | h_o | g_o | h_m | g_m |
| A | 11.4 | 192 | 10.9 | 192 | 10 | 45.6 | 10.2 | 47.4 |
| B | 10.9 | 195 | 10.6 | 190 | 10.1 | 46.6 | 10 | 45.8 |
| C | 11.4 | 191 | 10.8 | 192 | 10.3 | 44.6 | 10.2 | 47.6 |
| D | 9.53 | 174 | 9.51 | 166 | 8.70 | 28.2 | 8.29 | 28 |
| E | 11.2 | 189 | 11.8 | 192 | 10.3 | 40.6 | 10.9 | 44.9 |
| F | 9.44 | 187 | 8.66 | 185 | 8.56 | 40.5 | 8.31 | 44.6 |
| G | 11 | 190 | 11.2 | 191 | 10 | 42.9 | 10.3 | 45.1 |
| H | 10.7 | 188 | 11.3 | 185 | 10.3 | 36.3 | 10.2 | 40.8 |
| I | 11.5 | 192 | 10.9 | 191 | 10.1 | 44.1 | 10.2 | 47.1 |
| J | 11.1 | 191 | 10.6 | 193 | 9.92 | 45.8 | 9.98 | 48.3 |

Table 8 Statistical analysis of the surge model performance for the year 2003

| Location | Bias (m) | RMSE (m) | NRMSE | R^2 |
|-----------------|----------|----------|-------|-------|
| Millport (I) | −0.004 | 0.164 | 0.039 | 0.966 |
| Bangor (H) | −0.003 | 0.134 | 0.033 | 0.978 |
| Portpatrick (G) | −0.003 | 0.135 | 0.029 | 0.983 |
| Port Rush (D) | −0.001 | 0.112 | 0.043 | 0.943 |
| Port Erin (E) | −0.004 | 0.145 | 0.024 | 0.989 |

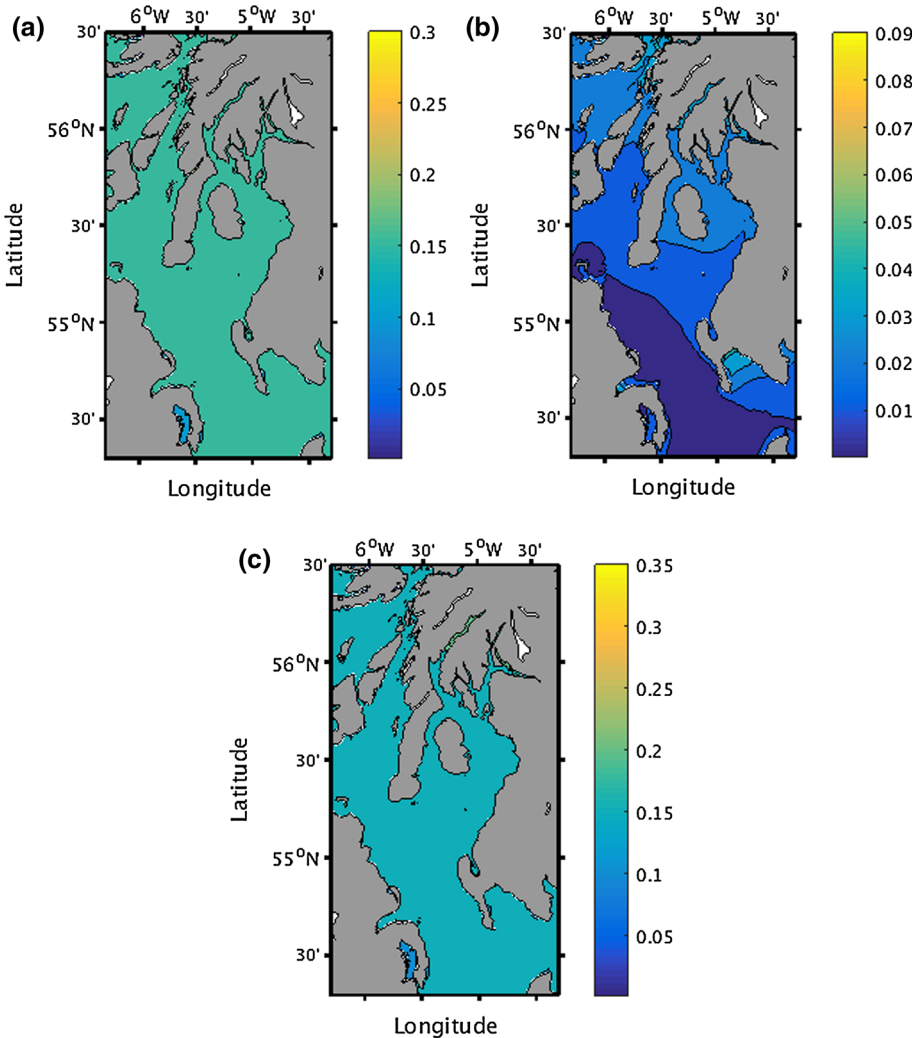


Fig. 9 Root-mean-square effect of different forcings on total water level (m): **a** Atlantic surges, **b** local wind and pressure, **c** combined effect. The RMSE was evaluated for the first figure as the difference of the simulation with surge boundaries and no local wind compared to a simulation with only tides, in the second case, the difference was between the wind and pressure only compared to the tidal simulation, while in the last case, we compared the total surge simulation with the tidal simulation. The RMSE was evaluated for the year 2003 (1 month spin-up in December 2002)

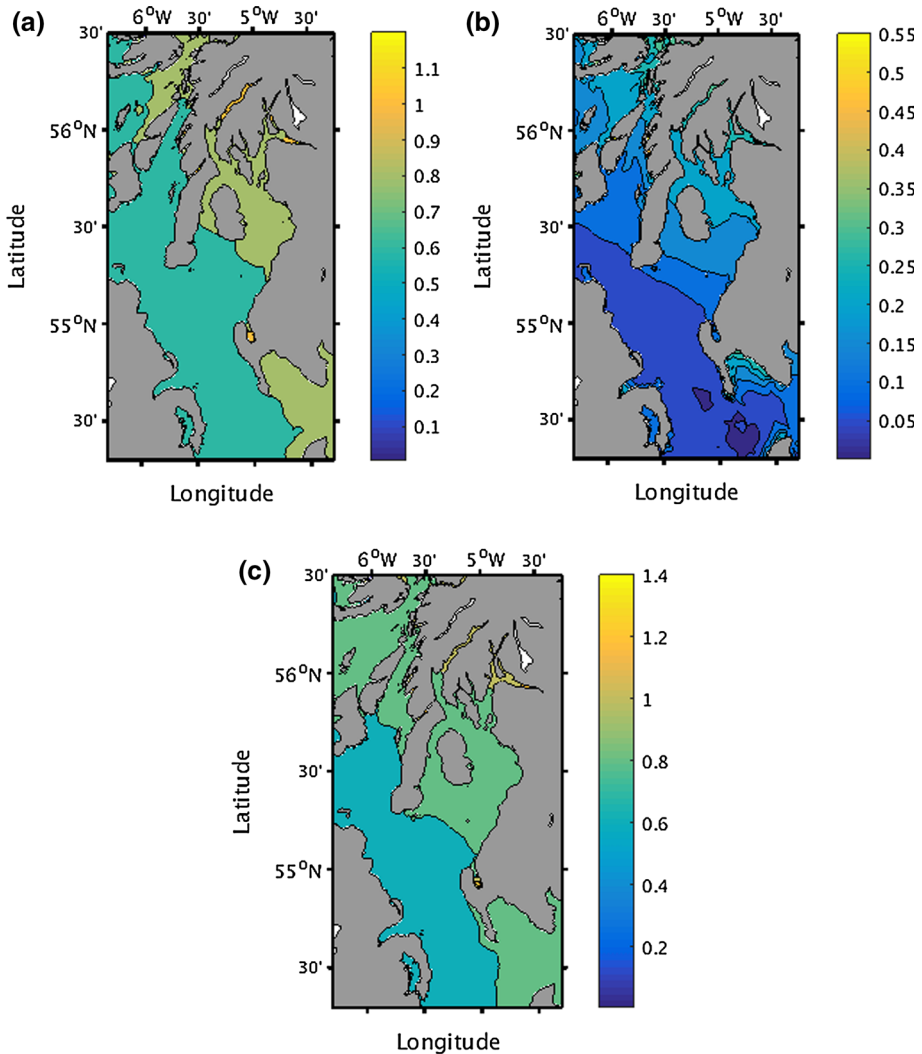


Fig. 10 Maximum modelled effect for different forcings on total water level (m): **a** Atlantic surges, **b** local wind and pressure, **c** combined effect. The maximum was evaluated for the first figure as the difference of the simulation with surge boundaries and no local wind compared to a simulation with only tides, in the second case, the difference was between the wind and pressure only compared to the tidal simulation, while in the last case, we compared the total surge simulation with the tidal simulation. The maximum difference was evaluated for the year 2003 (1 month spin-up in December 2002)

Collectively these findings, based on a 1-year run in both summer and winter conditions, indicate that the Clyde Sea areas most exposed to severe surges are the estuarine areas and the fjordic areas, in which the largest deviation from the astronomical tidal elevation are recorded. This suggests that the funnelling effects due to the complex coastline of the Clyde Sea are extremely important for the enhancement of the water level.

Our results also indicate that the North Channel is not as exposed as the Clyde Sea to severe surges, due to the deeper bathymetry: The increase in the surge wave is, in fact,

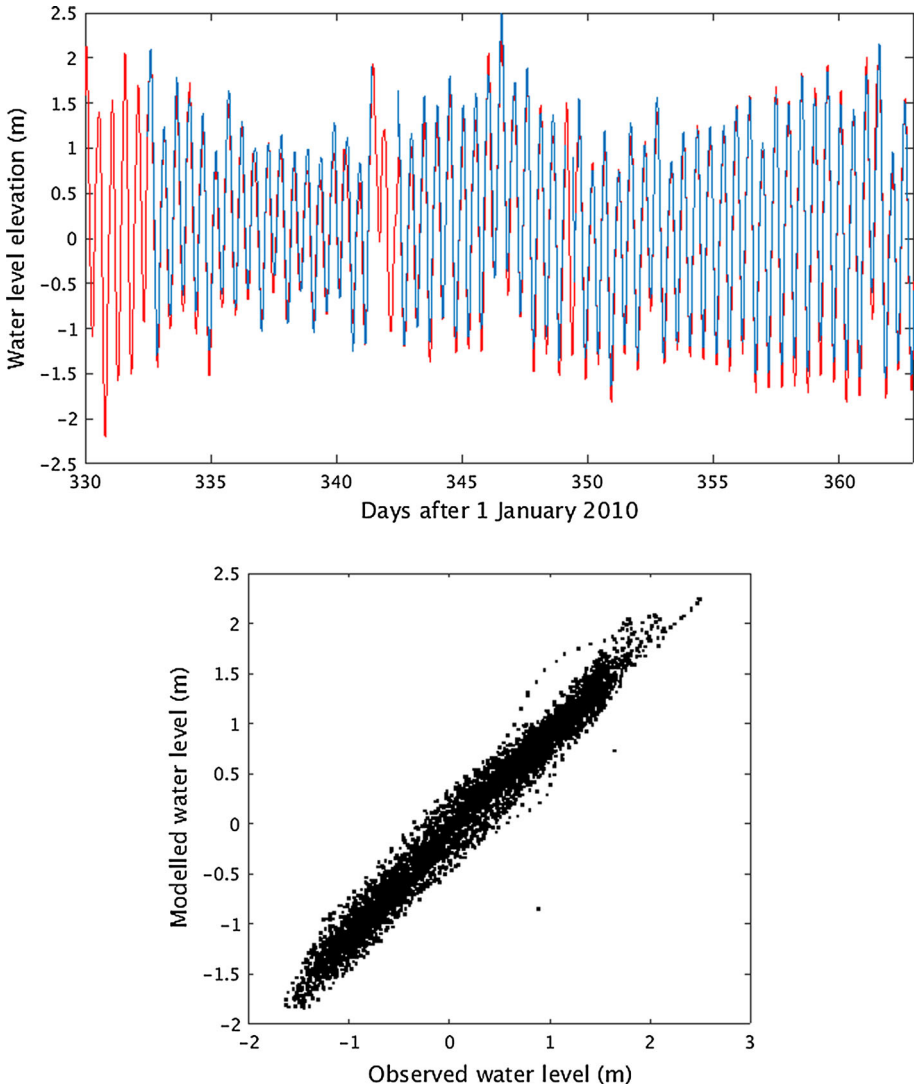


Fig. 11 Comparison between modelled and recorded water level and astronomical tide in Millport tide gauge for the month of December 2011; *red* is the modelled water level and *blue* is the observed water level

recorded in the shallow water area between the Clyde Sea and the North Channel. However, Figs. 9b and 10b show that in Belfast Lough, the local wind and pressure field can cause an enhancement greater than the surrounding North Channel (an average of 0.04 m, max effect of 0.25 m compared to the North Channel, that is an enhancement that can be compared to the Clyde Sea) due to the funnelling effect of the Belfast Lough on the surge wave. However, due to the location of the Belfast Lough, the Atlantic surge wave is not significantly amplified by the bathymetry or the coastline to be dangerous to the city of Belfast. In addition to this, the effect of the River Lagan is not considered in this study.

3.5 River contribution

To assess the contribution to sea level from river inflow, the model was run for the period in which the river inflow provided by SEPA was available (2005–2013). In particular, for this analysis, the year 2005 was considered. The results that we obtained from the simulation indicate that the water level enhancement due to the interaction between river, surge and tides was only significant in the inner part of the Clyde Estuary and did not have any far-field effect. No significant effects were found for the other rivers included in the simulation.

3.6 December 2011 storm surges

Three storms in December 2011 were hindcast to study the interaction between the surge wave and the tidal wave. The performance of the model was evaluated during December 2011 (Fig. 11; Table 9), and the model accurately predicted the total water level during this stormy period. Figures 12, 13 and 14 show the results of the model for the Clyde Sea at high water in Millport for each storm. For the first storm, the peak of the surge wave arrived after the maximum astronomical tide. In fact, the model hindcast shows a very strong enhancement of the water level in coincidence with the subsequent low astronomical tide (Fig. 12). Due to this lag between the peak storm wave and the high tide, as well as the coincidence with a neap tide period, the maximum total modelled water level did not exceed 2–2.5 m during the storm, despite a 1–1.5 m surge wave (Fig. 12b). The surge wave was effectively enhanced by the shallow bathymetry and the coastline of the sea lochs during this surge. The difference in height of the surge wave between the central part of the Clyde and the sealochs was 0.2–0.4 m. Nevertheless, in the northern sea lochs (Loch Fyne and the estuary of the Clyde in particular) and on the coastline near Ayr, some limited flooding events were reported. Unfortunately, the Millport tide gauge malfunctioned and did not record the peak period of the storm. The hydrodynamic model, in this case, was able to reconstruct the coupling between the surge wave tidal wave, predicting a surge wave exceeding 1 m in the Millport area. Conversely, in the North Channel, the surge never exceeded 1 m (Fig. 12b), and the maximum water level elevation was never >2 m (Fig. 12a).

The surge caused by Cyclone Hergen (Fig. 13) occurred at the same time as a spring tide period, so even though the surge wave was less intense than the one caused by Hurricane Bawbag, the total water level was higher, exceeding 2.5 m in the Clyde Sea and more than 3 m southward in the northern Irish Sea (Fig. 13a). This coupling between

Table 9 Statistical analysis of the surge model performance during November–December 2011. In Port Ellen tide gauge, there were no valid data for the comparison

| Location | Bias (m) | RMSE (m) | NRMSE | R^2 |
|-----------------|----------|----------|-------|-------|
| Millport (I) | −0.002 | 0.148 | 0.036 | 0.973 |
| Bangor (H) | −0.003 | 0.115 | 0.026 | 0.984 |
| Portpatrick (G) | 0.009 | 0.127 | 0.027 | 0.987 |
| Port Rush (D) | 0.003 | 0.084 | 0.033 | 0.970 |
| Port Ellen (F) | – | – | – | – |
| Port Erin (E) | 0.009 | 0.143 | 0.025 | 0.990 |
| Girvan (B) | −0.002 | 0.123 | 0.031 | 0.979 |
| Tarbert (C) | −0.007 | 0.311 | 0.062 | 0.889 |

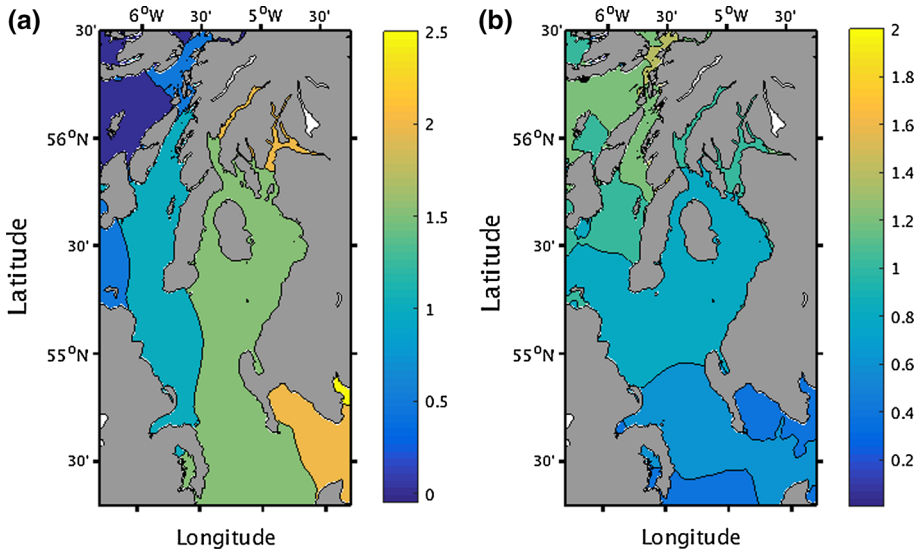


Fig. 12 Water level in the Clyde Sea at high water during Hurricane Bawbag: **a** total water level, **b** surge contribution

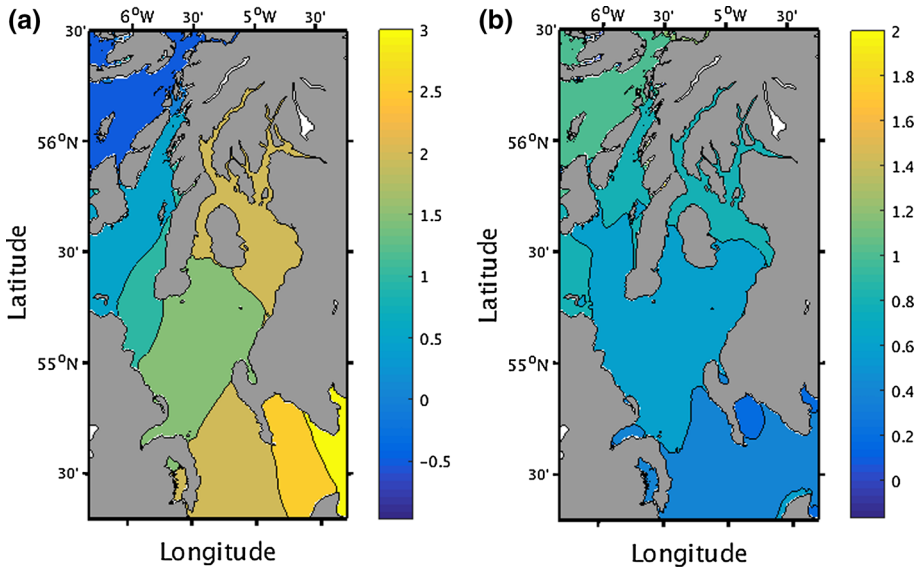


Fig. 13 Water level in the Clyde Sea at high water during Cyclone Hergen: **a** total water level, **b** surge contribution

strong surge and spring tides caused the flooding in many coastal communities in the Clyde Sea, in particular in Helensburgh.

The last storm (Fig. 2 for the photos of that day, Fig. 14 for the model results) was less intense than the other two storms analysed. Nevertheless, many coastal communities were

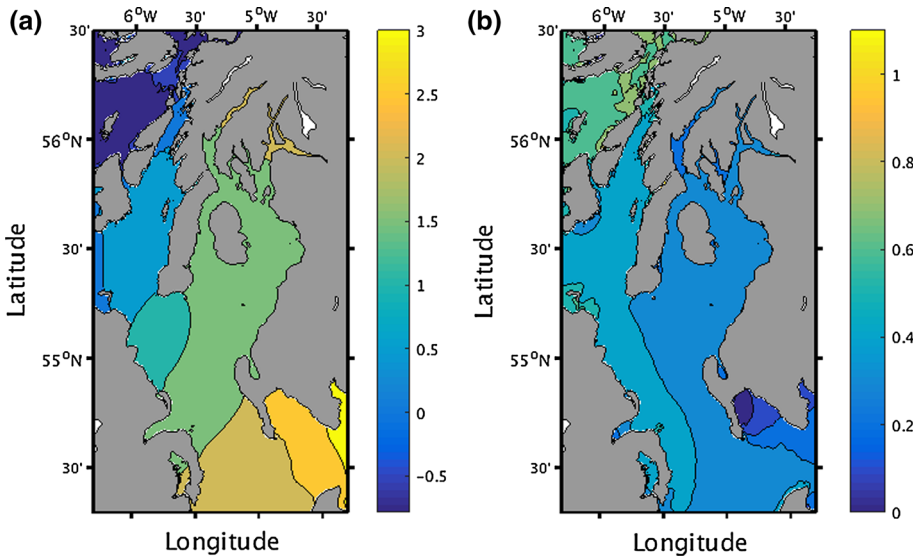


Fig. 14 Water level in the Clyde Sea at high water during the 28 December storm: **a** total water level, **b** surge contribution

still flooded, and much damage was recorded. The storm surge in the Clyde Sea never exceeded 1 m (Fig. 14b), but the spring tide conditions caused a high sea level in the sea lochs, in particular in the Clyde Estuary similar to the storm caused by the Hergen cyclone. This coupling caused another flood in streets near to the seafront in Helensburgh (Fig. 2).

3.7 River contribution during storm surges

The model was run in 2011 with and without river inflow and the output were compared in order to study the river effect on the total water level. For the first storm, the contribution of the rivers was very small: The Clyde river contributed up to 0.02 m in the estuary and in neighbouring areas, while no substantial contribution was coming from the other rivers. Also for the second storm, the maximum river contribution to storm surge was <0.01 m, while for the third storm was <0.02 m. In both cases, this contribution was from the Clyde river.

4 Conclusions

Our analysis of the historical tide gauge data showed that the highest water elevations in the Clyde Sea are recorded when spring high tides coincide with moderate to severe surge conditions, that from the statistical analysis in Fig. 7 usually occur during late autumn–winter. Approximately 90 % of storm surges with residuals >1 m were generated outside the Clyde Sea. The storms generating those events usually follow a particular pattern, with the low pressure from the Atlantic moving to the north of mainland Scotland or further north, over the Orkneys or the Fair Isle Channel. Only 8.9 % of storm surges exceeding 1 m can be explained by a low pressure over the Clyde or the North Channel.

The surge generation processes in the Clyde Sea contrast with mechanisms in other semienclosed basins around the world. In the Adriatic Sea, for example, large surges (such as *acqua alta* events in Venice) are internally generated by Bora or Scirocco winds (Orlić et al. 1994; Wakelin and Proctor 2002). Similarly, the majority of surges are internally generated in the Baltic Sea (Suursaar and Sooäär 2007), and in the Mediterranean Sea itself (Ullmann and Moron 2008). Other semienclosed basins, in fact, such as the bays in the west coast of the USA, are usually protected from surges from outside due to their complex coastline and bathymetry, such as Chesapeake Bay, and only very strong local winds can cause floods and large surges (Li et al. 2006). However, in all of these cases, the extent of the basin is larger than that in the Clyde, and/or the open ocean connecting channel is narrower and/or is oriented in the opposite direction to the climatological wind. The Clyde Sea is also a very particular semienclosed basin, if compared to the classification made by Pickard and Emery (Pickard and Emery 1990; Cessi et al. 2014), since it shows some features of the first case (single strait, exchange flow is separated vertically), and some of the second case (multiple straits, substantial net flow into/out of each strait). The Clyde Sea (joint with the North Channel) could be considered a semienclosed basin of the case B in the Pickard and Emery classification, since two entrances are present, but the Clyde Sea is separated from the North Channel due to an abrupt change in the bathymetry. All of these factors contribute to the peculiar surge climate of the Clyde Sea.

Our high-resolution model of the sea level dynamics in the Clyde Sea shows that the surge wave from the open boundaries is enhanced by the funnelling effect of the sealochs and estuary in the northern Clyde Sea and by the steep bathymetry at the entrance of the semienclosed basin. In addition, the external surge is often exacerbated by the local field of wind and pressure.

Our results illustrate these phenomena in greater detail than has been possible with previous surge models of the region (Townson and Donald 1985; Townson and Collar 1986; Kaya et al. 2005). The hindcasting of the three storms in the Clyde Sea during December 2011 corroborates the experience of coastal flooding patterns. In particular, the 28 December flooding event in the Inner Clyde was due to only a moderate surge wave, with residuals in Millport <0.6 m (Fig. 14), but this coincided with a spring high tide leading to an extreme total sealevel elevation.

The future development of this high-resolution model will be the operational stage, in which this model will be used for flood forecasting purposes, given the satisfactory results when used for surge hindcasting. This will be achieved through the nesting the model with a large-scale model and forecasted wind and pressure from an atmospheric model instead of the climatological wind.

Acknowledgments The authors would like to thank Alejandro Gallego, Sophie Elliot, Pierre Cazenave, Robert Wilson, Alessandra Romanó, Dmitry Aleynik, Judith Wolf, Ken Brink and Ian Thurlbeck for their support of the project and for their useful suggestions, and Gabriel Barrencea and The Centre for Numerical Algorithms and Intelligent Software (NAIS) for allowing us to use the NAIS cluster. The project was supported by the University of Strathclyde, Scottish Environment Protection Agency (SEPA) and Marine Scotland Science (MSS). The coastline for this paper is available at NOAA National Geophysical Data Center, GSHHG, under GNU Lesser General Public Licence, GEBCO bathymetry (GEBCO_08 Grid) is available at BODC website under copyright and database right restriction, SeaZone bathymetry is not publicly available, ©SeaZone Solutions, 2014, [Licence 022007.002]. Tide gauge data and RCMs used from this study are from Marine Scotland Science (MSS), UK Tide Gauge Network, Scottish Association for Marine Science (SAMS) and Centre for Environment, Fisheries and Aquaculture Science (CEFAS), provided by British Oceanographic Data Centre (BODC). Rothesay, Girvan, Tarbert and Campbeltown tide gauge data were provided by Scottish Environment Protection Agency (SEPA). Computer facilities were

supported by the Engineering and Physical Sciences Research Council of Great Britain under the Numerical Algorithms and Intelligent Software (NAIS) for the evolving HPC platform grant EP/G036136/1.

Open Access This article is distributed under the terms of the Creative Commons Attribution 4.0 International License (<http://creativecommons.org/licenses/by/4.0/>), which permits unrestricted use, distribution, and reproduction in any medium, provided you give appropriate credit to the original author(s) and the source, provide a link to the Creative Commons license, and indicate if changes were made.

References

- Aquaveo L (2007) SMS: Linear Interpolation
- Banks JC, Camp JV, Abkowitz MD (2014) Adaptation planning for floods: a review of available tools. *Nat Hazards* 70(2):1327–1337
- Cessi P, Pinardi N, Lyubartsev V (2014) Energetics of semienclosed basins with two-layer flows at the strait. *J Phys Oceanogr* 44(3):967–979
- Chen C, Liu H, Beardsley RC (2003) An unstructured grid, finite-volume, three-dimensional, primitive equations ocean model: application to coastal ocean and estuaries. *J Atmos Ocean Technol* 20(1):159–186
- Chen C, Beardsley RC, Cowles G (2006) An unstructured grid, finite-volume coastal ocean model (FVCOM) system. *Oceanography* 19(1):78
- Chen C, Cowles G, Beardsley R (2006) An unstructured grid, finite-volume coastal ocean model: FVCOM user manual. SMASST/UMASSD
- Codiga DL (2011) Unified tidal analysis and prediction using the UTide Matlab functions. Graduate School of Oceanography, University of Rhode Island, Narragansett
- Cowles GW (2008) Parallelization of the FVCOM coastal ocean model. *Int J High Perform Comput Appl* 22(2):177–193
- Davies AM, Hall P, Howarth MJ, Knight P, Player R (2001) A detailed comparison of measured and modeled wind-driven currents in the North Channel of the Irish Sea. *J Geophys Res Oceans* (1978–2012) 106(C9):19683–19713
- Davies AM, Hall P, Howarth MJ, Knight PJ, Player RJ (2004) Tidal currents, energy flux and bottom boundary layer thickness in the Clyde Sea and North Channel of the Irish Sea. *Ocean Dyn* 54(2):108–125
- Davies AM, Hall P (1998) The sensitivity of tidal current profiles in the North Channel of the Irish Sea to the parameterization of momentum diffusion. *Cont Shelf Res* 18(2):357–404
- Davies AM, Hall P (2000) The response of the North Channel of the Irish Sea and Clyde Sea to wind forcing. *Cont Shelf Res* 20(8):897–940
- Dee D, Uppala S, Simmons A, Berrisford P, Poli P, Kobayashi S, Andrae U, Balmaseda M, Balsamo G, Bauer P et al (2011) The ERA-Interim reanalysis: configuration and performance of the data assimilation system. *Q J R Meteorol Soc* 137(656):553–597
- Dietrich G (1950) Die natürlichen Regionen von Nord-und Ostsee auf hydrographischer Grundlage. *Kieler Meeresforsch* 7(2):35–69
- Egbert GD, Erofeeva SY, Ray RD (2010) Assimilation of altimetry data for nonlinear shallow-water tides: quarter-diurnal tides of the northwest european shelf. *Cont Shelf Res* 30(6):668–679. doi:10.1016/j.csr.2009.10.011. <http://www.sciencedirect.com/science/article/pii/S02784343090%03094>. (Tides in Marginal Seas - A special issue in memory of Prof Alexei Nekrasov)
- Ferziger JH, Perić M (2002) Computational methods for fluid dynamics, vol 3. Springer, Berlin
- Fisher R, Jantsch M, Comer R (1982) General bathymetric chart of the oceans (gebco). Canadian Hydrographic Service, Ottawa
- Hankin B, Lewis A, Robinson, ALP, Henderson D, Lancashire S, Wells S (2008) A spatial understanding of significant flood risk in Northern Ireland using social, economic and environmental flood risk metrics based on fluvial, coastal, pluvial and historical flooding. In: Irish national hydrology conference, Tullamore, vol 11
- Hickey KR (2001) The storm of 31 January to 1 February 1953 and its impact on Scotland. *Scott Geogr Mag* 117(4):283–295
- Kaya Y, Stewart M, Becker M (2005) Flood forecasting and flood warning in the Firth of Clyde, UK. *Nat Hazards* 36(1–2):257–271
- Li M, Zhong L, Boicourt WC, Zhang S, Zhang DL (2006) Hurricane-induced storm surges, currents and destratification in a semienclosed bay. *Geophys Res Lett* 33(2):L02604. doi:10.1029/2005GL024992

- Matthews J, Buchholz F, Saborowski R, Tarling G, Dallot S, Labat J (1999) On the physical oceanography of the Kattegat and Clyde Sea area, 1996–98, as background to ecophysiological studies on the planktonic crustacean, *Meganyctiphanes norvegica* (Euphausiacea). *Helgol Mar Res* 53(1):70–84
- Olbert AI, Hartnett M (2010) Storms and surges in Irish coastal waters. *Ocean Model* 34(1):50–62
- Orford J, Murdy J (2015) Presence and possible cause of periodicities in 20th-century extreme coastal surge: Belfast Harbour, Northern Ireland. *Glob Planet Chang* 133:254–262
- Orlić M, Kuzmić M, Pasarić Z (1994) Response of the Adriatic Sea to the bora and sirocco forcing. *Cont Shelf Res* 14(1):91–116
- Pawlowicz R (2000) *M_Map: a mapping package for Matlab*. University of British Columbia Earth and Ocean Sciences. [Online]. <http://www.eos.ubc.ca/rich/map.html>
- Pickard GL, Emery WJ (1990) *Descriptive physical oceanography: an introduction*. Elsevier, Boston
- Pingree R, Holligan P, Mardell G (1978) The effects of vertical stability on phytoplankton distributions in the summer on the northwest European Shelf. *Deep Sea Res* 25(11):1011–1028
- Pingree R, Griffiths D (1979) Sand transport paths around the British Isles resulting from M 2 and M 4 tidal interactions. *J Mar Biol As UK* 59(02):497–513
- Rego J, Li C (2009a) On the receding of storm surge along Louisiana's low-lying coast. *J Coast Res* 115:1045–1049
- Rego JL, Li C (2009b) On the importance of the forward speed of hurricanes in storm surge forecasting: a numerical study. *Geophys Res Lett* 36(7):L07609. doi:10.1029/2008GL036953
- Rego JL, Li C (2010a) Nonlinear terms in storm surge predictions: effect of tide and shelf geometry with case study from Hurricane Rita. *J Geophys Res Oceans* (1978–2012) 115(C6):C06020. doi:10.1029/2009JC005285
- Rego JL, Li C (2010b) Storm surge propagation in Galveston Bay during hurricane Ike. *J Mar Syst* 82(4):265–279
- Rippeth T, Simpson J (1996) The frequency and duration of episodes of complete vertical mixing in the Clyde Sea. *Cont Shelf Res* 16(7):933–947
- Rodi W (1993) *Turbulence models and their application in hydraulics*. CRC Press, Boca Raton
- Simpson J, Rippeth T (1993) The Clyde Sea: a model of the seasonal cycle of stratification and mixing. *Estuar Coast Shelf Sci* 37(2):129–144
- Smagorinsky J (1963) General circulation experiments with the primitive equations: I. The basic experiment*. *Mon Weather Rev* 91(3):99–164
- Suursaar Ü, Sooäär J (2007) Decadal variations in mean and extreme sea level values along the Estonian coast of the Baltic Sea. *Tellus A* 59(2):249–260
- Townson J, Collar R (1993) Assessment of the potential of a coastal flood warning scheme for the Firth of Clyde. Report to Clyde River Purification Board
- Townson JM, Collar RH (1986) Water movement and the simulation of storm surges in the Firth of Clyde. *Environ Estuary Firth Clyde Proc R Soc Edinb B* 90:87–96
- Townson J, Donald A (1985) Numerical modelling of storm surges in the Clyde Sea area. In: *ICE proceedings*, vol 79, pp 637–655. Thomas Telford
- Ullmann A, Moron V (2008) Weather regimes and sea surge variations over the Gulf of Lions (French Mediterranean coast) during the 20th century. *Int J Climatol* 28(2):159
- Versteeg HK, Malalasekera W (2007) *An introduction to computational fluid dynamics: the finite volume method*. Pearson Education, New York
- Wakelin S, Proctor R (2002) The impact of meteorology on modelling storm surges in the Adriatic Sea. *Glob Planet Chang* 34(1):97–119
- Weisberg RH, Zheng L (2008) Hurricane storm surge simulations comparing three-dimensional with two-dimensional formulations based on an Ivan-like storm over the Tampa Bay, Florida region. *J Geophys Res Oceans* (1978–2012) 113(C12):C12001. doi:10.1029/2008JC005115
- Werritty A, Houston D, Ball T, Tavendale A, Black A (2007) Exploring the social impacts of flood risk and flooding in Scotland. Scottish Executive, Edinburgh
- Wessel P, Smith WH (1996) A global, self-consistent, hierarchical, high-resolution shoreline. *J Geophys Res* 101:8741–8743